Available online at www.sciencedirect.com
SCIENCE DIRECT
International Journal of Mass Spectrometry 251 (2006) 252–259
International Journal of Mass Spectrometry
www.elsevier.com/locate/ijms

Studies of neutron-rich isotopes with the CPT mass spectrometer and the CARIBU project

G. Savard [a,b,*], J.C. Wang [a,c], K.S. Sharma [c], H. Sharma [a,c], J.A. Clark [a,c], C. Boudreau [a,d], F. Buchinger [d], J.E. Crawford [d], J.P. Greene [a], S. Gulick [d], A.A. Hecht [a,e], J.K.P. Lee [d], A.F. Levand [a], N.D. Scielzo [a], W. Trimble [a], J. Vaz [a], B.J. Zabransky [a]

[a] *Physics Division, Argonne National Laboratory, Argonne, IL 60439, USA*
[b] *Department of Physics, University of Chicago, Chicago, IL 60637, USA*
[c] *Department of Physics and Astronomy, University of Manitoba, Winnipeg, Man., Canada R3T 2N2*
[d] *Department of Physics, McGill University, Montreal, Que., Canada H3A 2T8*
[e] *Department of Chemistry, University of Maryland, College Park, MD 20742, USA*

Received 2 January 2006; received in revised form 30 January 2006; accepted 31 January 2006

Abstract

The heavy neutron-rich isotopes area is the least explored region of the nuclear landscape. Although sensitive techniques exist to gather the required information on these isotopes, they just have not been made available in sufficient quantity and with the right properties for many of the most basic studies. Recent measurements at the Canadian Penning trap (CPT) mass spectrometer, using isotopes produced from the fission of ^{252}Cf stopped in the CPT gas catcher system, have allowed the mass of a number of neutron-rich isotopes to be determined. This approach is being further pursued in the CARIBU project with the installation of a new dedicated heavily shielded source and gas catcher that will yield four orders of magnitude higher neutron-rich isotope yield at low energy for mass measurements and Coulomb barrier energy for nuclear structure studies.

PACS: 21.10.Dr; 27.60.+j; 27.70.+q; 29.25.Rm

Keywords: Mass measurement; Penning trap; Neutron-rich isotopes

1. Introduction

Our understanding of nuclear structure has evolved in stages, frequently driven by technological advances. Initial mass measurement capabilities [1] indicated the presence of stable isotopes of the different elements. Light-ion induced reactions [2] then allowed the investigation of these stable nuclei and the resultant explosion of new information stimulated the development of the shell model [3] and collective models [4]. Accelerated heavy ions [5] allowed us to move away from the valley of stability and progress to very high spin. The curvature of the valley of stability allowed roughly a 1000 new proton-rich isotopes to be studied. Again, this wealth of information stimulated theory and a new generation of mean field models and techniques for cranking the mean field to understand the effects of fast rotation. We are in a new phase. In theory, the development of ab initio methods [6] has moved our understanding of the structure of light nuclei onto an entirely new quantitative plane with strong predictive power and high precision. In experiment, the challenge of very neutron-rich nuclei with completely new topologies such as neutron halos and skins has been glimpsed at, and accelerated radioactive beams are seen as the practical way to make progress.

The neutron-rich "terra incognita" in which thousands of isotopes lie, and about which we know little, has already been shown to be full of surprises. At the dripline, where binding is the weakest, extensive "halos" [7] of low density neutron matter have been found in light nuclei. In several cases the dripline was found to extend further than expected. Nearer stability, strong modification to the normal sequence of single-particle states [8] has been observed, leading to new shell gaps and new shapes. There are also strong indications, from the isotope production

* Corresponding author. Tel.: +1 630 252 4024; fax: +1 630 252 6210.
E-mail address: savard@anl.gov (G. Savard).

1387-3806/$ – see front matter © 2006 Elsevier B.V. All rights reserved.
doi:10.1016/j.ijms.2006.01.047

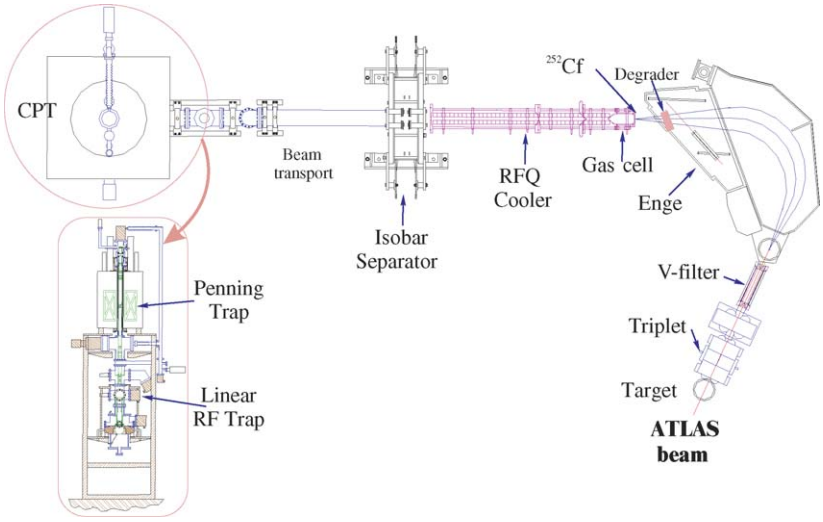

Fig. 1. Schematic of the CPT mass spectrometer and its injection system.

in the r-process for example, that the pronounced shell structure we are familiar with close to stability is altered in weakly bound neutron-rich systems. Standard nuclear reactions tend to populate the proton-rich side of the nuclear chart and, as a result, the neutron-rich region of the nuclear chart has remained mostly uncharted. Exploring the far reaches of this region is a key component of the low-energy scientific programs of planned future facilities such as RIA and FAIR. And while the full capabilities of those facilities will be required to thoroughly explore this region, interesting forays in this new territory would yield extremely useful information provided intense neutron-rich isotope beams at low energies and Coulomb barrier energies were available.

In recent years, mass measurements of short-lived neutron-rich isotopes have been performed at the Canadian Penning trap (CPT) spectrometer at Argonne. These isotopes were obtained from a ^{252}Cf source with the fission fragments stopped in the gas catcher system developed at the CPT, thermalized there and subsequently injected into the measurement trap system. While this allows to reach isotopes more neutron-rich than available before and illustrates the universality of the approach, it is still limited in scope by the strength of the fission source that can be used safely in the existing CPT injection system. Overcoming this limitation requires a dedicated properly shielded source holder and gas catcher system. This is the approach chosen in the CARIBU californium source upgrade to ATLAS where a four orders of magnitude stronger source than that used at the CPT will be used to provide an array of neutron-rich radioactive beams, including isotopes that have not been amenable to ISOL techniques before, at sufficient energy and intensity to provide information on the key nuclear properties and help delineate some of the parameters required for the future research programs.

The sections below give a description of the CPT spectrometer and present some of the results on neutron-rich heavy isotopes obtained this far. This is followed by a brief description of the CARIBU project and the capabilities it will provide for mass measurements and other studies on neutron-rich isotopes.

2. The CPT mass spectrometer

A schematic view of the CPT mass spectrometer system is shown in Fig. 1. The instrument can be divided into three main parts by function: (i) the production of ions, (ii) the preparation of ions for measurement, and (iii) the measurement of the mass of the selected ions.

2.1. Production of ions

The CPT can measure the masses of ions produced either on-line or off-line. In the on-line mode, nuclei created through fusion–evaporation reactions recoil out of the target and are focused onto the entrance of a gas catcher [9]. In the off-line mode that is used in this work, a 45 μCi ^{252}Cf fission source is placed close to the gas catcher window. Fission fragments that pass through the 1.9 mg/cm^2 Havar entrance window are thermalized in 200 mbar of purified helium gas and subsequently guided by the gas flow and radio frequency (RF) and dc electric fields to a RFQ cooler.

2.2. Preparation of ions for measurement

The RFQ cooler consists of four segmented rods that form an ion guide [10,11]. The structure is divided into three sections by apertures to reduce the gas pressure from 200 mbar of helium at the exit of the gas catcher to 10^{-4} mbar in the last RFQ section. RF voltages applied to the rods form an oscillating quadrupole field that produces a transversely focusing force. The segmented rods allow the superposition of a dc voltage gradient along the axis of the device to guide the ions forward. Ions lose transverse and longitudinal energy due to collisions with the residual helium gas as they pass through the structure. They are finally accumulated in a potential well formed by the last three segments of the ion guide. The ions are then ejected, as ion bunches, by applying appropriate voltage pulses to these segments.

The ion bunches are then captured and mass analyzed in the isotope separator [12,13]. The isotope separator is a gas-filled

Penning trap consisting of nine electrodes with cylindrical geometry and is located in the bore of a 1.0 T electromagnet. dc voltages are applied to these electrodes to obtain an electrostatic quadrupole field in the center of the trap. The central ring electrode is split into quadrants to allow the application of dipole and quadrupole RF fields. The ion motion due to this superposition of the homogeneous magnetic field and the electrostatic quadrupole field is a combination of three harmonic eigenmotions [14,15]: an axial oscillation along the magnetic field axis at a frequency ω_z, and a magnetron and modified cyclotron motion in the radial plane with frequencies ω_- and ω_+, respectively. In general, ω_- is much smaller than ω_+, but these two frequencies are related to the true cyclotron frequency ω_c of the ions by the relation $\omega_c = \omega_+ + \omega_-$. As a result of the dissipative force provided by the collisions of the ions with the helium buffer gas, the amplitude of the modified cyclotron motion decays much faster than the growth of the magnetron motion amplitude. A quadrupole radio frequency field with frequency ω_c is applied on the ring electrode which converts the magnetron motion to the modified cyclotron motion. The modified cyclotron motion is subsequently lost due to collisions with the buffer gas. Thus, ions can be cooled and centered in the trap [12,15]. The process is mass selective and is used for the elimination of unwanted ion species. The remaining ions are then ejected out of the isotope separator and transferred through an electrostatic beam transport system to the CPT. Since the isotope separator does not remove all of the contaminant ions with different masses, a fast voltage pulse, applied to one of the beam transport elements, efficiently further suppresses isotopes outside a restricted range of masses.

The ions transferred from the isotope separator are captured, accumulated, and cooled in a linear RF trap. This trap is similar to the trap at the end of the RFQ cooler and consists of four rods segmented into three parts, with helium buffer gas (at a pressure of 10^{-4} mbar) introduced into the trap through a needle valve. This trap allows the accumulation and cooling of several ion bunches which are then injected into the precision Penning trap. The relatively long measurement cycle in the precision trap ($\sim$1 s) can thus be decoupled from the 20 Hz ejection rate from the RFQ cooler (or the 2 Hz rate from the isotope separator after its installation). The cooling afforded by the collisions with the buffer gas ensures that ions are always injected into the precision Penning trap with identical initial properties.

A number of electrostatic steerers and Einzel lenses are used to guide and focus the ions during their transport from the RFQ cooler to the precision Penning trap. Along this flight path, at various positions, microchannel plate (MCP) detectors are used to diagnose ion beams and surface barrier silicon detectors are used to monitor β activity.

The precision Penning trap itself is located in the bore of a 5.9 T superconducting magnet. The basic electrode configuration of the trap consists of two endcaps and a central ring electrode which describe hyperboloids of revolution and follow the equipotential surfaces of the quadrupole field. The ring electrode is also segmented into quarters to allow the application of dipole and quadrupole RF fields superimposed on the electrostatic fields to drive the ion motions, in a similar fashion to the isotope separator but without the presence of a buffer gas. A set of correction electrodes are included to compensate for the gaps and apertures that any practical arrangement must include. All of the materials used in the construction of the vacuum chamber and the trap are compatible with high-vacuum requirements and have little effect on the magnetic field.

To minimize systematic effects, the captured ions are subjected to two processes. First, an "evaporation pulse" is applied to momentarily reduce the trapping potential from its nominal value. This allows ions with relative high kinetic energy to escape axially. When the trapping potential returns to its normal value only the ions that occupy a small volume in the center of the trap are left. Second, electric dipole radio frequency fields are applied on the split ring electrode at the modified cyclotron frequencies of contaminant ions. In this manner, it is possible to increase the orbital radius of these undesired ions and remove them from the trap. The remaining ions consist almost entirely of the desired species and occupy a small volume near the center of the trap, a condition necessary for the precise measurement of their true cyclotron frequency.

2.3. Measurement of the cyclotron frequency of the selected ions

A three-step process is used for the precise mass measurement of the selected ions. First, a dipole field at the magnetron frequency excites the ions to a preset magnetron orbital radius. This process is relatively insensitive to the mass of the ion and is consistently used to ensure that both calibrant and unknown ions move in similar magnetic fields. Second, a RF quadrupole electric field is applied for a preset duration. If the applied frequency of the quadrupole field corresponds to the cyclotron frequency (ω_c) of the trapped ions, the initial slow magnetron motion is converted to the faster modified cyclotron motion with similar radius [14,15]. Finally, the ions are ejected out of the Penning trap. As they drift through the magnetic field gradient of the superconducting magnet, the orbital energy gained is converted to axial energy through the interaction of the orbital magnetic moment with the magnetic field gradient. A MCP detector, installed at the end of the TOF section, is used to detect the ions and their arrival time is recorded with a multichannel scaler. The entire process is repeated for successive ion bunches as the frequency of the applied quadrupole field is scanned, in equal increments, over a preset range of frequencies. A complete set of TOF spectra, one for each frequency, constitutes a single scan. Many scans are taken and the spectra averaged.

The cyclotron frequencies and their statistical uncertainties are obtained by determining the position of the minimum in the TOF spectra since the ions trapped in the Penning trap gain the most energy when driven by a quadrupole field at the cyclotron frequency, and therefore arrive at the MCP detector in the least amount of time [16]. The TOF spectra are fitted [17] with a modified sine function $(\sin(x)/x)$ with five adjustable parameters, a good approximation to the true line profile discussed in [15]. The resonant frequency of the doubly charged neutron-rich isotopes investigated here is about 1.2 MHz. With the application of a quadrupole electric field for 500 ms, the Fourier limit for the full width at half the maximum amplitude

Table 1
Table of the determined mass and uncertainty for the 26 neutron-rich isotopes measured

Isotope	Mass of neutral species (μu)	Uncertainty (μu)	σ deviation from AME95	σ deviation from AME03
^{141}Ba	140914396.5	7.5	−0.9	−1.3
^{142}Ba	141916423.2	9.1	−2.2	−2.7
^{143}Ba	142920625.0	8.5	0.5	−0.1
^{144}Ba	143922954.7	9.1	0.8	0.1
^{145}Ba	144927518.4	9.1	9.2	−1.4
^{146}Ba	145930282.5	23.7	2.0	0.8
^{147}Ba	146935303.9	21.2	12.9	1.6
^{143}La	142916081.9	8.7	1.2	1.0
^{144}La	143919662.9	19.3	1.1	1.1
^{145}La	144921811.2	13.3	2.3	1.7
^{146}La*	145925817.5	30.6	1.4	0.3
^{147}La	146928417.8	11.5	7.1	3.5
^{148}La	147932679.4	20.9	3.5	6.7
^{145}Ce	144917228.2	92.2	0.0	−0.1
^{146}Ce	145918808.2	20.8	1.6	0.7
^{147}Ce	146922690.8	9.6	3.0	0.5
^{148}Ce	147924421.8	13.0	0.2	−0.3
^{149}Ce	148928426.9	11.0	1.7	0.3
^{150}Ce	149930381.4	13.1	1.2	−0.5
^{151}Ce	150934272.2	19.0	0.7	2.6
^{148}Pr*	147922260.7	30.6	0.8	3.0
^{149}Pr	148923736.1	10.6	−3.5	0.2
^{150}Pr	149926677.1	10.6	−3.7	0.1
^{151}Pr	150928302.5	14.3	1.8	−0.6
^{152}Pr	151931552.9	19.9	−0.1	0.4
^{153}Pr	152933889.5	15.3	0.7	0.5

Also given are the deviation from AME95 and AME03 for each isotope. Isomeric contamination can be present for the isotope marked with an asterisk (∗) symbol (see text).

(FWHM) of the cyclotron resonances, $\Delta\nu_c = 0.89/T_{RF}$ [14], is approximately 1.8 Hz. This corresponds to a resolving power of $R = \nu_c/\Delta\nu_c(\text{FWHM}) = 7 \times 10^5$ (or approximately 220 keV at $A = 150$).

Masses are obtained by measuring the cyclotron frequencies of both the nuclide of interest and a calibrant ion of well-known mass. The mass of the investigated isotope is then found from the cyclotron frequency ratio ν_{ref}/ν_{ion}, between the cyclotron frequency of the singly charged molecular ions used here (with subscript 'ref') and that of the doubly charged ions of the isotopes studied (with subscript 'ion') via the relation

$$m_{ion} = 2(m_{ref} - m_e)\nu_{ref}/\nu_{ion} + 2m_e,$$

with m_e the electron mass.

3. Initial results on neutron-rich isotopes

A survey of the ions produced from the heavy ^{252}Cf fission fragment peak indicated that most of the activity was collected as doubly charged ions. The cyclotron frequencies of 26 of these doubly charged nuclides, namely $^{141-147}$Ba^{2+}, $^{143-148}$La^{2+}, $^{145-151}$Ce^{2+}, and $^{148-153}$Pr^{2+}, were measured. Molecular ions composed of C, H, O, and N atoms are extracted from the gas catcher together with the radioactive ions and were used as calibrants.

An estimate of the total system efficiency can be made by considering the following. For the 45 μCi ^{252}Cf source used, the production rate for ^{143}Ba is 2.2k atoms/s [18]. The gas catcher is optimized for online operation with fusion–evaporation reactions so that in the case of fission we estimate that only approximately 3% of the fragments stop in the gas catcher. The number of ^{143}Ba ions detected on the final MCP TOF detector was 2.1 s^{-1}. Therefore, the efficiency of the system from the source to detection on the final MCP detector was approximately 10^{-3}.

All isotopes were measured more than once along with reference molecules of similar mass to calibrate the magnetic field. The final masses are determined from the weighted average of all data. Most of the measurements for the same isotope are in agreement within their respective uncertainties, but for the few cases in which they are not, the uncertainty in the weighted average is inflated by the square root of the reduced χ^2. Table 1 lists the isotopes measured, the final masses and uncertainties, together with the differences from the 1995 Atomic-Mass Evaluation (AME95) [19] and the 2003 Atomic-Mass Evaluation (AME03) [20].

The contributions from known sources of systematic errors were determined. These include the masses of the calibrants used, the stability of the magnetic field, and the number of ions stored in the trap. The masses of the molecular ions used as calibrants have constituent masses (C, H, N, O) known to typically better than 1 part in 10^{10} and total mass uncertainty limited by the uncertainty of their respective molecular binding energy. These calibrating masses are known to about two orders of magnitude better precision than those obtained here for the short-lived isotopes so that the calibration is essentially absolute. They form a

convenient calibration network, just as precise as carbon clusters (the uncertainty also limited by the binding energy), but available at essentially all masses. Therefore, the precision of our magnetic field calibration is limited by our measurement of the cyclotron frequencies of the reference ions and not by the intrinsic uncertainty of their mass. The stability of the magnetic field has been measured during these measurements to be much better than 1 part in $10^9\,h^{-1}$. This is in agreement with the observation in [17,21,22].

The systematic uncertainty due to the number of ions of the selected species during each measurement cycle has been studied in detail for our instrument [21]. The effect determined in this work agrees with that in [21] and is found to be no larger than 2 parts in 10^9 per detected ion. The systematic uncertainty due to the number of contaminant ions stored in the Penning trap during each measurement cycle has also been investigated. A comparison of our results prior to and after the installation of the isotope separator shows that the effect is not larger than 2×10^{-8} of the mass per detected contaminant ion. Since all mass measurements were taken within a few hours of calibration, and only a few ions were trapped in the Penning trap for each measurement cycle, the systematic uncertainty under these conditions has been conservatively estimated at 4×10^{-8} of the mass studied and is dominated by the possible presence of contaminants. The final mass uncertainty is obtained by adding the systematic uncertainty and the statistical uncertainty in quadrature and is listed in Table 1. The total uncertainty is found to be dominated by the limited statistics accumulated for the radioactive nuclides.

Our results are compared to the masses from AME95 in the top part of Fig. 2. The masses of $^{141-144}$Ba in the literature are from high-precision mass measurements performed by ISOLTRAP [23]. The good agreement between our measured masses and those from [23], obtained with very different production and injection techniques and different trapping systems, indicates that it is unlikely that either the ISOLTRAP or the CPT measurements suffer from unaccounted systematic errors. For these isotopes, our measured masses agree with AME03 except for ^{142}Ba where our value (and that from [23]) is lower than the accepted value. When moving to more exotic nuclei than those that have been measured in [23], we find much larger deviations. As shown in Table 1, deviations between 1σ and 3σ are observed for ^{146}Ba, $^{143-146}$La, ^{146,147,149,150}Ce, and ^{151}Pr. Extreme discrepancies are observed for ^{145}Ba (9σ), ^{147}Ba (12σ), ^{147}La (7σ), ^{148}La (3.5σ), and ^{149,150}Pr (4σ), whose masses were previously determined through Q_β measurements [24,25]. Such measurements, especially for heavier nuclei where the decay schemes are quite complicated, are often susceptible to systematic errors. The disagreements observed are believed to be mainly due to incorrect β-endpoint energy measurements or underestimated uncertainties.

Our measured masses are compared with the masses from AME03 in the bottom of Fig. 2. The agreement between our measurements and AME03 is improved significantly in comparison with AME95, especially for ^{145,147}Ba, ^{147}La, ^{147}Ce, and ^{149,150}Pr. For these isotopes, AME03 included new measurements [26,27] and rejected some older results [24] that were included in AME95. Large deviations are still seen for ^{147}Ba, ^{147,148}La, and ^{151}Ce, the most neutron-rich isotopes reached by this work.

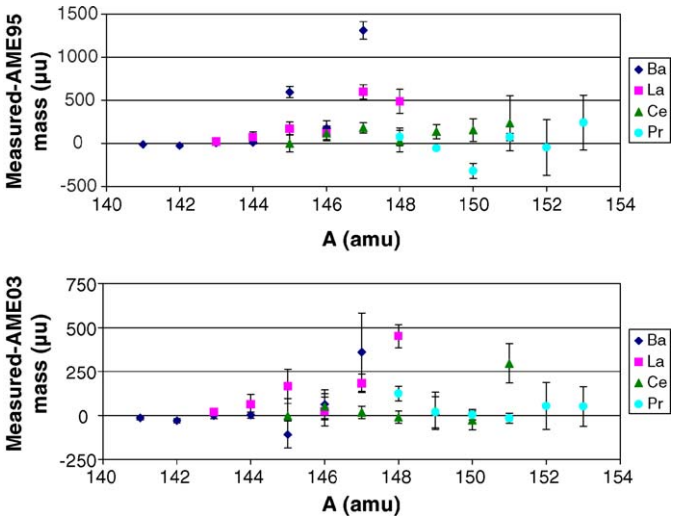

Fig. 2. Comparison between the results obtained here and the 1995 and 2003 mass tabulations.

Of the 26 isotopes studied here, isomeric states with a lifetime long enough to be present during measurement are known to be present only in ^{148}Pr and ^{146}La [28]. NUBASE [29] gives excitation energies of 50(30) and 130(130) keV for ^{148}Pr and ^{146}La, respectively, and the ground states have not been identified. The CPT operated at a nominal resolving power of ≃200 keV for these measurements. Since the excitation energy is smaller than our line width, our measured masses of ^{148}Pr and ^{146}La should be interpreted as the average of the masses of the isomeric and ground states weighted by their (unknown) relative intensities. However, our mass for ^{146}La is in excellent agreement with the value quoted in AME03 (see Table 1). Two Q_β values, ^{146}Ba$(\beta_-)^{146}$La and ^{146}La$(\beta_-)^{146}$Ce play a significant role in determining the mass of ^{146}La in AME03. Each Q_β value in AME03 is the average of two disparate inputs: 4030(50) keV [24] and 4280(100) keV [30] for ^{146}Ba$(\beta_-)^{146}$La; 6620(70) keV [24] and 6380(70) keV [31] for ^{146}La$(\beta_-)^{146}$Ce. The differences between the two input Q_β values, for each of these decays, are consistent with each other (with an average value of 245(74) keV). Our data yields a Q_β value of 4160(34) keV for ^{146}Ba$(\beta_-)^{146}$La and a value of 6529(34) keV for ^{146}La$(\beta_-)^{146}$Ce. The sums of the Q_β values for these two decays, from each of these sources and AME03 as well, agree with each other indicating that the mass difference between ^{146}Ba and ^{146}Ce is consistently reproduced. We suggest that the differences between the individual Q_β values show the influence of the long-lived (>5 s) isomeric state in ^{146}La. If one interprets that the results of [24] only involved the isomeric state and that those reported in [30] and [31] involved only the ground state, then one can deduce an excitation of 245(74) keV for the isomeric state. Our value for the mass of ^{146}La would therefore represent a mixture of both ground and isomeric states with a $55 \pm 29\%$ excited

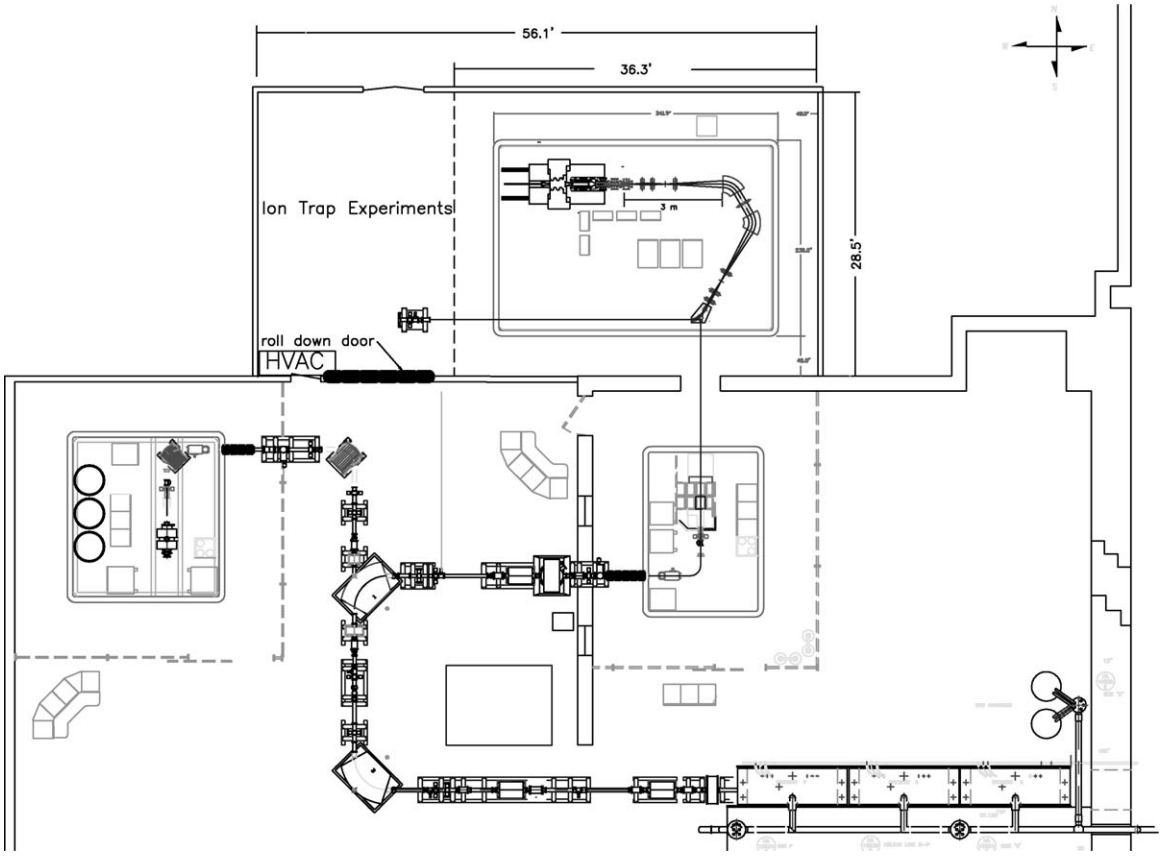

Fig. 3. Layout for the CARIBU project with the new building (top part of the figure) hosting the new high-voltage platform. The CPT spectrometer will be moved to the adjacent experimental area to make measurements on the high intensity low-energy neutron-rich beams extracted from the new platform.

state population. For ^{148}Pr, our value differs significantly from that given in AME03. The previous measurements accepted into AME03 consist of two independent β-endpoint measurements that link ^{148}Pr with ^{148}Nd. These two values are consistent with each other and their average value is relatively unchanged from the evaluation in AME03. However, our value for the mass of ^{148}Pr is heavier than AME03 by 125(41) μu, a difference that is too large to be explained entirely by the suggested value for the excitation energy of the isomeric state alone.

It is observed that the most neutron-rich isotopes measured here were much less bound (heavier) than predicted by the AME95 extrapolations, and are still significantly less bound than the AME03 values. Measurements are currently underway using a 500 μCi source to determine if this trend is confirmed as we move further away from stability. The additional yield will also allow higher resolution to be used to separate isobars when present.

To reach more neutron-rich isotopes in this region, in particular those on the r-process path which depends critically on the isotope masses, much higher yield is required. This implies a new capture system with a geometry better suited to stopping fission fragments and enough shielding to protect users from the neutrons from a ^{252}Cf source of roughly 1 Ci strength. The CARIBU project at ATLAS is being built to meet these requirements and is briefly introduced below.

4. The CARIBU project

The CARIBU californium source upgrade project to the ATLAS facility at Argonne aims to provide beams to increase the present knowledge of the neutron-rich region of the chart of nuclides. The task involves enabling experiment with beams of short-lived neutron-rich isotopes at low and Coulomb barrier energy regimes. Capabilities exist for radioactive beams in this region at other facilities but limitations in the species that can be extracted and the energy to which they can be accelerated hamper the ability of these facilities to address a number of key physics questions. The ATLAS facility at Argonne has unique capabilities and expertise to perform this research with a modest upgrade while demonstrating in battle conditions many of the technologies that are critical for future facilities such as RIA.

The necessary steps to accomplish the task are: (1) the production of the short-lived isotopes, (2) the rapid extraction and preparation of the selected isotopes, (3) their post-acceleration to the optimum energy for the particular experiment, and finally (4) the availability of the required instrumentation to carry out the experiments. The techniques developed at ATLAS for the CPT trapping program and for the RIA facility enable the stopping of fast recoil ions into a gas catcher and their rapid extraction as a low-energy beam of very good quality. This technique is applicable to essentially all species and is very efficient. Such a

gas catcher will be used to stop recoils from a 1 Ci ^{252}Cf fission source and to extract them as a low-energy beam. This provides access to all species produced in the fission of californium. In particular, this puts within reach species which are difficult to extract by standard ISOL techniques and are not produced with low-energy fission of uranium. This approach therefore provides unique beams that will not be available elsewhere at low energy until facilities like RIA come along.

The californium source and gas catcher will be located, together with an RFQ gas cooler and an isotope separator, on a new high-voltage platform. This new platform will be located in a new building (see Fig. 3) beside the existing ECR-1 high-voltage platform and have an independent high voltage control with output that can be compared and adjusted versus the ECR-1 high voltage. The extracted isotopes are transported and cooled in two sections of RFQ gas coolers yielding beams with very low transverse emittance and energy spread. The beams are then accelerated to 50 keV and sent to a high-resolution mass separator where a specific isotope is selected. The very good beam properties extracted from the gas cooler allows one to obtain a mass resolution of 20,000 with a one-stage separator that is a scaled down version of the isobar separator that has been designed for low-energy beam purification [32] at RIA. Two beamlines will be attached to the isobar separator; a low-energy beamline for tuning/diagnostics and low-energy experiments such as mass measurements, and a beamline leading to the existing ECR-1 high-voltage platform. Most unwanted activity will be stopped in the mass separator and remain on the first high-voltage platform. This platform is expected to be the only location where sizable accumulation of radioactive isotopes will occur.

Post-acceleration of the low-energy beams extracted from the first platform must be done efficiently. A charge-state breeder will be used to increase the charge state of the singly charged radioactive ions so that they can be accelerated directly in ATLAS. This will provide an acceleration route to the existing experimental area for physics at the Coulomb barrier. The ECR-1 ion source will be modified to be used as a charge-state breeder (it will remain usable as an ECR source for normal ATLAS operations). The mass selected singly (or doubly) charged ions will be injected into the ECR-1, their charge state increased by the plasma, and they will then be extracted and sent to ATLAS in a fashion identical to normal stable beams.

Only minor modifications to ATLAS will be implemented for this upgrade. The energy range accessible at ATLAS is sufficient to address the physics questions, mainly single-particle structure and pairing interaction in neutron-rich nuclei. Transmission of the ATLAS accelerator is very high, limited in theory only by the bunching efficiency that should be up to 85% with the multi-harmonic buncher currently in use. Diagnostics will also be improved in the injection into ATLAS to obtain better tunes for standard beams and extend their usefulness to lower intensity beams.

Finally, ATLAS already possesses first class instrumentation for most of the studies being proposed with the CPT spectrometer for mass measurements with the low-energy beams, and Gammasphere, the FMA and the Ludwig detector array and Enge spectrographs for experiments with accelerated beams.

The low-energy beams should be available early in 2008. The CPT spectrometer will be moved to the low-energy experimental area in the new building (see Fig. 3) and can start mass measurements on these new isotopes at that time. With the yields expected [33], precise mass measurements should be possible on about 200 new very neutron-rich isotopes that have not been amenable to Penning trap mass measurements previously.

Acknowledgements

This work was supported by the U.S. Department of Energy, Nuclear Physics Division, under Contract W-31-109-ENG-38 and grants from the Natural Sciences and Engineering Research Council of Canada. The authors are also indebted to the Office of Basic Energy Sciences, U.S. Department of Energy, for the use of the ^{252}Cf source, through the transplutonium element production facilities at the Oak Ridge National Laboratory. The help of Dr. Irshad Ahmad for preparation of the source is also acknowledged.

References

[1] J.J. Thomson, Phil. Mag. 24 (209) (1912) 668.
[2] S.T. Butler, Proc. R. Soc. A 208 (1951) 559.
[3] M.G. Mayer, Phys. Rev. 74 (1948) 235.
[4] A. Bohr, B.R. Mottelson, Phys. Rev. 90 (1953) 717.
[5] E. Almqvits, D.A. Bromley, J.A. Kuchner, Phys. Rev. Lett. 4 (1960) 515.
[6] S.C. Pieper, R.B. Wiringa, Annu. Rev. Nucl. Part. Sci. 51 (2001) 53 (and references therein).
[7] I. Tanihata, H. Hamagaki, O. Hashimoto, S. Nagamiya, Y. Shida, N. Yoshikawa, O. Yamakawa, K. Sugimoto, T. obayashi, D.E. Greiner, N. Takahashi, Y. Nojiri, Phys. Lett. B 160 (1985) 380.
[8] J. Dobaczewski, W. Nazarewicz, Prog. Theor. Phys. Suppl. 146 (2003) 70.
[9] J. Clark, R.C. Barber, K.S. Sharma, J. Vaz, J.C. Wang, C. Boudreau, F. Buchinger, J.E. Crawford, S. Gulick, J.K.P. Lee, R.B. Moore, J.C. Hardy, J.A. Caggiano, A. Heinz, G. Savard, D. Seweryniak, G. Sprouse, Nucl. Instrum. Meth. Phys. Res. B 204 (2003) 487.
[10] M. Maier, C. Boudreau, F. Buchinger, J.A. Clark, J.E. Crawford, J. Dilling, H. Fukutani, S. Gulick, J.K.P. Lee, R.B. Moore, G. Savard, J. Schwartz, K.S. Sharma, Hyperfine Interact. 132 (2001) 521.
[11] F. Herfurth, J. Dilling, A. Kellerbauer, G. Bollen, S. Henry, H.-J. Kluge, E. Lamour, D. Lunney, R.B. Moore, C. Scheidenberger, S. Schwarz, G. Sikler, J. Szerypo, Nucl. Instrum. Meth. Phys. Res. A 469 (2001) 254.
[12] G. Savard, St. Becker, G. Bollen, H.-J. Kluge, R.B. Moore, T. Otto, L. Schweikhard, H. Stolzenberg, U. Wiess, Phys. Lett. A 158 (1991) 247.
[13] H. Raimbault-Hartmann, D. Beck, G. Bollen, M. Koenig, H.-J. Kluge, E. Schark, S. Schwarz, J. Szerypo, Nucl. Instrum. Meth. Phys. Res. B 126 (1997) 378.
[14] G. Bollen, R.B. Moore, G. Savard, H. Stolzenberg, J. Appl. Phys. 68 (1990) 4355.
[15] M. Koenig, G. Bollen, H.-J. Kluge, T. Otto, J. Szerypo,, Int. J. Mass Spectrom. Ion Process. 142 (1995) 95.
[16] G. Gräff, H. Kalinowsky, J. Traut, Z. Phys. A 297 (1980) 35.
[17] G. Savard, J.A. Clark, F. Buchinger, J.E. Crawford, S. Gulick, J.C. Hardy, V.E. Iacob, J.K.P. Lee, A.F. Levand, B.F. Lundgren, N.D. Scielzo, K.S. Sharma, I. Tanihata, I.S. Towner, W. Trimble, J.C. Wang, Z. Zhou, Phys. Rev. C 70 (2004) 042501(R).
[18] T.R. England, B.F. Rider, Los Alamos National Laboratory Report LA-UR-94–3106, 1994.
[19] G. Audi, A.H. Wapstra, Nucl. Phys. A 595 (1995) 409.
[20] G. Audi, A.H. Wapstra, C. Thibault, Nucl. Phys. A 726 (2003) 337.
[21] J.V.F. Vaz, Ph.D. Thesis, University of Manitoba, 2002.
[22] G. Savard, F. Buchinger, J.A. Clark, J.E. Crawford, S. Gulick, J.C. Hardy, A.A. Hecht, J.K.P. Lee, A.F. Levand, N.D. Scielzo, H. Sharma, K.S.

Sharma, I. Tanihata, A.C.C. Villari, Y. Wang, Phys. Rev. Lett. 95 (2005) 102501.
[23] F. Ames, G. Audi, D. Beck, G. Bollen, M. de Saint Simon, R. Jertz, H.-J. Kluge, A. Kohl, M. Koenig, D. Lunney, I. Martel, R.B. Moore, T. Otto, Z. Patyk, H. Raimbault-Hartmann, G. Rouleau, G. Savard, E. Schark, S. Schwarz, L. Schweikhard, H. Stolzenberg, J. Szerypo, the ISOLDE collaboration, Nucl. Phys. A 651 (1999) 3.
[24] M. Graefenstedt, U. Keyser, F. Münnich, F. Schreiber, AIP Conf. Proc. 164, Nucl. Far From Stability 5th Int. Conf., Rosseau Lake, Ontario, Canada, 1987.
[25] M. Graefenstedt, P. Juergens, U. Keyser, F. Muennich, F. Schreiber, K. Balog, T. Winkelmann, H.R. Faust, B. Pfeiffer, Z. Phys. A 336 (1990) 247.
[26] C. Weber, Ph.D Thesis, Heidelberg, 2003.
[27] T. Ikuta, A. Taniguchi, H. Yamamoto, K. Kawade, Y. Kawase, J. Phys. Soc., Jpn. 64 (1995) 3244.
[28] R.B. Firestone, Table of Isotopes, 8th ed., Wiley, New York, 1996.
[29] See http://csnwww.in2p3.fr/amdc/web/nubase_en.html.
[30] R. Decker, K.D. Wuensch, H. Wollnik, G. Jung, J. Muenzel, G. Siegert, E. Koglin, Z. Phys. A 301 (1981) 165.
[31] D.S. Brenner, M.K. Martel, A. Aprahamian, R.E. Chrien, R.L. Gill, H.I. Liou, M. Schmid, M.L. Stelts, A. Wolf, F.K. Wohn, D.M. Rehfield, H. Dejbakhsh, C. Chung, Phys. Rev. C 26 (1982) 2166.
[32] M. Portillo, J.A. Nolen, T.A. Barlow, in: P. Lucas, S. Webber (Eds.), Proceedings of the 2001 IEEE Particle Accelerator Conference, vol. 1, Chicago, IL, June 18–22, 2001, p. 3015.
[33] See http://www.phy.anl.gov/atlas/caribu.html.